Pergamon

Bioorganic & Medicinal Chemistry, Vol. 5, No. 8, pp 1555–1567, 1997
Published by Elsevier Science Ltd
Printed in Great Britain

PII: S0968-0896(97)00100-4

0968-0896/97 $17.00 + 0.00

In Vivo Muscarinic Binding Selectivity of (*R,S*)- and (*R,R*)-[^{18}F]-Fluoromethyl QNB

Dale O. Kiesewetter,* Richard E. Carson, Elaine M. Jagoda, Christopher J. Endres, Margaret G. Der, Peter Herscovitch and William C. Eckelman

National Institutes of Health, Positron Emission Tomography Department, Warren G. Magnusen Clinical Center, 10 Center Drive, Bethesda, MD 20892-1180, U.S.A.

Abstract—We have developed a multistep radiochemical synthesis of two diastereomers of quinuclidinyl-4-[^{18}F]-fluoromethyl-benzilate ([^{18}F]-FMeQNB), a high-affinity ligand for muscarinic acetylcholine receptors. Previously, we have shown that the nonradioactive (*R,R*)-diastereomer displays an eightfold selectivity for M1 over M2 while the nonradioactive (*R,S*)-diastereomer displays a sevenfold selectivity for M2 over M1 in vitro. This paper reports the results of in vivo comparison studies. In the rat, uptake of (*R,S*)-[^{18}F]-FMeQNB was nearly uniform in all brain regions following the concentration of M2 subtype. The uptake was reduced by 36–54% in all brain regions on coinjection with 50 nmol of unlabeled ligand. An injection of (*R,S*)-[^{18}F]-FMeQNB followed at 60 min by injection of unlabeled ligand and subsequent sacrifice at 120 min displaced 30–50% of radioactivity in the pons, medulla, and cerebellum, which contain a high proportion of M2 subtype. The most dramatic displacement and inhibition of uptake on coinjection of (*R,S*)-[^{18}F]-FMeQNB was observed in the heart. In rhesus monkey, the compound showed prolonged uptake and retention in the brain. In the blood, the parent compound degraded rapidly to a single radiolabeled polar metabolite believed to be fluoride. Within 30 min the parent compound represented less than 5% of the plasma activity. Displacement with (*R*)-QNB was generally slow, but was more rapid from those tissues which contain a higher proportion of M2 subtype. The results are consistent with the hypothesis that (*R,S*)-[^{18}F]-FMeQNB is M2 selective in vivo. On the other hand, (*R,R*)-[^{18}F]-FMeQNB showed higher uptake in those brain regions containing a higher concentration of M1 subtype. Uptake in the heart at 60 min was much lower than that observed with the (*R,S*)-diastereomer. Inhibition of uptake on coinjection with unlabeled (*R,S*)-FMeQNB is only significant in the heart, thalamus, and pons. Inhibition of uptake on coinjection with unlabeled (*R,R*)-FMeQNB is quite uniform in all brain regions. Displacement with (*R*)-QNB shows a more varying amount displaced. These results are consistent with (*R,R*)-[^{18}F]-FMeQNB being M1 selective in vivo. Published by Elsevier Science Ltd.

Introduction

Muscarinic acetylcholine receptors are one of several classes of receptors that couple to G proteins and exhibit a regulatory function. Pharmacologically four subtypes (M1, M2, M3, and M4) have been described based on differential affinity to various ligands. Five discrete muscarinic receptors have been identified and cloned: m1, m3, and m5 are linked to phosphoinositol turnover; m2 and m4 are coupled to adenylate cyclase. The pharmacological subtypes and the cloned subtypes display high correlation.[1,2] Throughout this manuscript we shall use the 'M' designation without distinguishing cloned from pharmacological subtypes, because our primary evidence for subtype selectivity is based on pharmacological subtype binding assays.

The distribution of muscarinic subtypes in rats has been determined by a combination of methods and has been summarized by Gitler et al. in nanomolar concentration units (nM).[3] M2 receptor has a fairly uniform distribution throughout the brain (27–39 nM) with the exception of the cerebellum where its concentration is about half (15 nM). By contrast, M1 sites are distributed heterogeneously.

Our interest in subtype-selective ligands for the M2 site stems from the observation that the pharmacological M2 receptor concentration is reduced in cortical brain regions of patients with Alzheimer's disease studied post-mortem.[4,5] Flynn et al. studied post-mortem Alzheimer's brains with antibodies for the muscarinic acetylcholine subtypes[6] and found decreased M2 subtype concentration in the frontal cortex of 43%. There was also a decreased M1 subtype concentration in the frontal, temporal, and parietal cortex of about 30%; however, the B_{max} for pirenzepine, the prototypical M1 specific ligand for in vitro assays, is unchanged from controls.

Our goal is to develop an M2 selective ligand that crosses the blood brain barrier and can be labeled with fluorine-18, a positron-emitting radionuclide. Such a radioligand may be useful in the determination of M2 receptor numbers in brain of living patients by positron emission tomography (PET). The results from PET studies may confirm or refute the post-mortem observations of M2 loss in cortical regions and perhaps, determine if the loss is a cause or a consequence of the disease process. In addition, M1 subtype selective

Address correspondence to Dale O. Kiesewetter, Ph.D.; NIH/CC/PET, Building 10 Room 1C495, 10 Center Drive MSC 1180, Bethesda, MD 20892-1180, U.S.A. Phone: 301-435-2229. Fax: 301-402-3521. E-mail: dk7k@nih.gov

ligands are also desired to investigate the reported change of this subtype in Alzheimer's disease.

A number of radiolabeled muscarinic acetylcholine ligands have been prepared and studied using PET. In addition, other radiopharmaceuticals for studying various aspects of central cholinergic neurotransmission have been studied with PET and single photon emission computed tomography (SPECT). This work has been the subject of a recent review.[7] PET investigators have studied ^{11}C analogues of acridine,[8] benztropine,[9] dexetimide,[10] QNB,[11] *N*-methyl scopolamine,[12] and tropanyl benzilate.[13] Isomeric ^{18}F analogues of dexetimide have been prepared.[14] All of these PET ligands are reported to have poor subtype selectivity. Recently, the M1 selective ligand xanomeline (3-[4-(hexyloxy)-1,2,5-thiadiazol-3-yl]-1,2,5,6-tetrahydro-1-methylpyridine), which is being evaluated as a potential therapy for Alzheimer's dementia, and its butylthio analogue have been labeled with C-11 and studied in PET.[15] Several stereoisomers of quinuclidinyl α-(iodo-2-propenyl)-α-hydroxyphenyl acetate have been studied for subtype selectivity in both labeled and unlabeled forms.[16–18] Two diastereomers of IQNB [quinuclidinyl 4-iodobenzilate]-and the parent (*R*)-QNB have been compared for their subtype selectivity. While (*R,S*)-IQNB displayed an in vivo distribution in brain proportional to the total muscarinic receptor concentration,[19] the parent (*R*)-QNB is M2 selective.[20,21]

There have been two approaches to the development of an M2 selective imaging agent. One is to base the structure on AF-DX 116 [11-(((2-(diethylamino)-methyl)-1-piperidinyl)acetyl)-5-11-dihydro-6H-pyrido-(2,3b)(1,4)benzodiazepin-6-one], which shows M2 selectivity in vitro but does not cross the blood–brain barrier, and modify the structure to improve brain uptake without losing selectivity.[3,22] The other approach is to conduct synthetic modifications of IQNB, which crosses the blood brain barrier but exhibits low selectivity, and examine the resultant selectivity profile.[17,18,23,24] Here we present our results following this latter approach.

Quinuclidinyl benzilate (QNB) analogues have been studied because of their muscarinic antagonist properties. This molecule has one chiral center in the quinuclidine ring (Scheme 1).

The higher biological activity is possessed by the *R* enantiomer. When analogues are synthesized, which contain a single substitution at an aromatic position, a second chiral center is generated at the benzilic carbon. In our stereochemical nomenclature (*R,R*), the first letter refers to the absolute stereochemistry at the quinuclidinyl center; the second letter is the absolute stereochemistry at the benzilic center. Prior to the initiation of our studies, only stereoisomers of IQNB had been studied. Our synthetic studies and the subsequent analysis of the absolute configuration revealed that the assignment of stereochemistry of IQNB had been in error.[25]

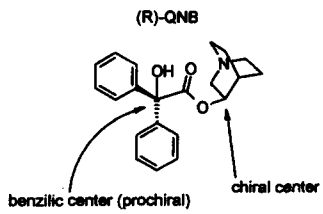

Scheme 1.

We previously reported the stereoselective synthesis of fluorine-containing analogues of quinuclidinyl benzilate (QNB) [23] and the in vitro subtype selectivity of (*R,S*)- and (*R,R*)-FMeQNB. (*R,S*)-FMeQNB ((*R*)-quinuclidinyl-(*S*)-4-[^{18}F]-fluoromethylbenzilate) shows a 7:1 selectivity of M2 over M1, while (*R,R*)-FMeQNB ((*R*)-quinuclidinyl-(*R*)-4-[^{18}F]-fluoromethylbenzilate) shows an 8:1 selectivity of M1 over M2. In vivo, 50 nmol of (*R,S*)-FMeQNB inhibits uptake of [^{125}I]-(*R,R*)-IQNB to a greater extent in tissues with a higher proportion of M2 subtype, consistent with M2 selectivity.[26] Autoradiographic studies also support M2 selectivity in vivo.[27]

In this paper we present the results of in vivo studies with both (*R,R*)- and (*R,S*)-[^{18}F]-FMeQNB. Additional co-administration and displacement studies were conducted in rats to show the reversibility in binding. We also conducted biodistribution and displacement studies in monkeys utilizing (*R,S*)-[^{18}F]-FMeQNB and PET.

Results and Discussion

Synthesis of precursors for labeling

Syntheses of the authentic (*R,R*)- and (*R,S*)-fluoromethyl QNB (FMeQNB) analogues and their in vitro affinity profiles have been published.[23] The radiosynthesis required an alternative approach in which the fluorine-18 could be introduced at a later stage in the radiosynthesis because of its 110 min half-life. Although 4-hydoxymethyl QNB could be prepared, attempts to activate the 4-benzylic alcohol as the mesylate and subsequently displace with fluoride were unsuccessful. The mesylate was formed in the reaction mixture and survived extraction into $CHCl_3$. However, during or after evaporation of the solvent the product decomposed and the resulting residue was observed to be insoluble in $CHCl_3$. An alternate procedure was developed in order to have stable precursors.

Precursors for fluoride displacement were synthesized using the previously published asymmetric method[23] which utilizes (1*R*,2*S*,5*R*)-5-methyl-2-(1-methyl-1-phenylethyl)cyclohexanol (8-phenylmenthol) as chiral auxiliary. (*S*)-4-Hydroxymethyl benzilic acid 8-phenylmenthyl ester (**1**), prepared as previously described,[23] was hydrolyzed to the corresponding benzilic acid (**2**) (Scheme 2). (*R*)-4-Hydroxymethyl benzilic acid (**9**, Scheme 3) was prepared in an analogous manner.

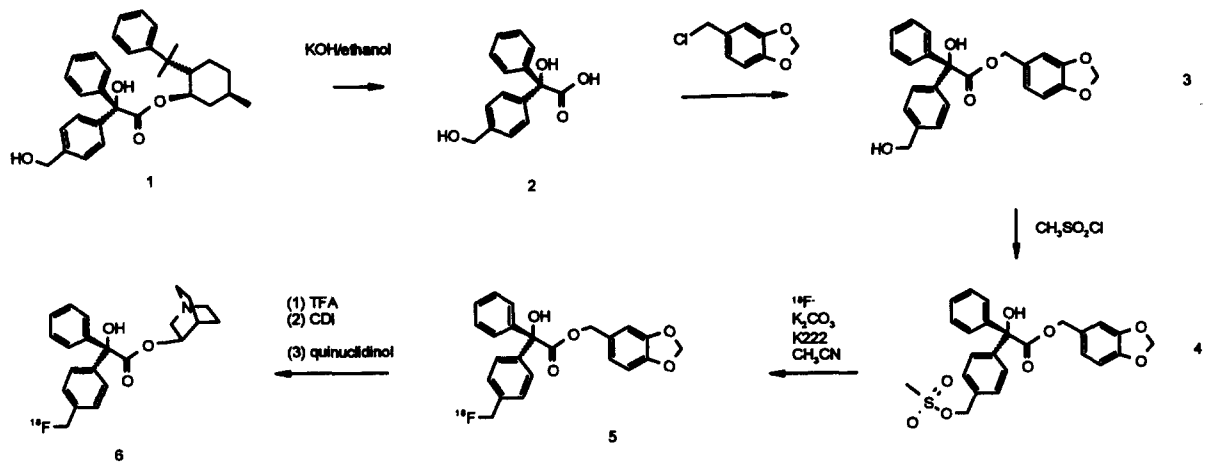

Scheme 2.

8-Phenylmenthyl 4-methyl benzoyl formate (**7**) was prepared from the corresponding acid chloride and 8-phenylmenthol. Reaction of **7** with phenylmagnesium bromide at −78 °C gave 8-phenylmenthyl (*R*)-4-methyl benzilic acid. 8-Phenylmenthyl (*R*)-4-bromomethyl-benzilic acid was prepared by benzylic bromination of this 4-methyl precursor. The bromomethyl derivative was converted to the alcohol (**8**) by treatment with silver trifluoroacetate followed by aqueous work up. The hydroxymethyl ester was subsequently hydrolyzed to the desired (*R*)-hydroxymethyl benzilic acid (**9**). The hydroxymethyl benzilic acids (**2** and **9**) were converted into their respective asymmetric precursors for labeling as demonstrated for **2** in Scheme 2. (*S*)-4-Hydroxy-methyl benzilic acid was protected as the acid labile[28] piperonyl ester (**3**) and the benzylic alcohol activated for nucleophilic substitution by conversion to the mesylate (**4**).

Radiochemistry

For radiosynthesis, a three-step procedure was developed (Scheme 2) which parallels that of the unlabeled synthesis of (*S*)-fluoromethyl benzilic acid.[23] The mesylate was displaced by [^{18}F]-fluoride in good yield using K_2CO_3/Kryptofix in CH_3CN. The product was eluted through silica with CH_2Cl_2 and evaporated. The piperonyl ester was hydrolyzed by treatment with trifluoroacetic acid. Coupling of the resulting acid with (*R*)-quinuclidinol was accomplished using carbonyl diimidazole following the procedure for synthesis of [^{11}C]-QNB.[29] The radiochemical yield, based on initial

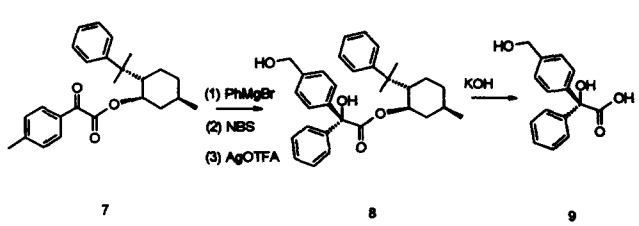

Scheme 3.

[^{18}F]-fluoride, after isolation from the HPLC eluant was 8.2 ± 2.3% (uncorrected for radionuclide decay) on successful syntheses (n = 23). The total time of the synthesis was approximately 70 min. The measured specific activity ranged from 339 to 5077 mCi/μmol EOB (n = 16).

Product stability in vitro

During the in vivo studies in rats and rhesus monkeys described below, we observed the compound to exhibit decomposition. The decomposition is demonstrated by the appearance of a radioactive component with an R_f of 0. It is presumed to be [^{18}F]-fluoride based on the R_f, the known propensity for benzylic fluorides to hydrolyze,[30,31] and the observed uptake into bone. In rats the bone uptake was about 1% ID/g at 120 min. The stability of [^{18}F]-FMeQNB was studied in vitro following the standard procedure for metabolite analysis (see the Experimental section) in saline, various aqueous buffers, in rat blood and in rhesus monkey blood. The stability in saline from batch to batch was variable and we were unable to determine the cause. Some preparations showed high stability regardless of handling (radiochemical purity >95% at 60 min). One batch displayed a decrease to 80% radiochemical purity over 2 h in saline, but showed stability in 50 mM NaH_2PO_4 (pH ~ 5) over the same 2-h period. The stability of [^{18}F]-FMeQNB was also variable in monkey plasma.

The amount of decomposition was lower in rat blood compared to monkey blood. Since the only other experimental difference was the presence of anesthesia, we evaluated the stability as a function of anesthesia. We could not establish any effect on defluorination from the ketamine, atropine, and pentothal used in the animals prior to the PET study. We did observe a small increase in decomposition in blood from monkeys which were under isoflurane anesthesia compared to the same monkeys prior to isoflurane. However, we can not establish significance. We also evaluated the effect of temperature of incubation on the decomposition and

observed no difference in the amount of decomposition at 37 °C compared to room temperature or 0 °C.

(*R,S*)-[^{18}F]-FMeQNB in rats

Biodistribution of (*R,S*)-[^{18}F]-FMeQNB and the effects of competing ligands were studied in rats. Because of the differences in the percent injected dose per gram tissue observed between studies with different preparation of the radioligand, comparisons were made only between control and test group animals from the same date. We chose 50 nmol/rat as the dose of competing ligand because our previous studies showed this dose most clearly defined subtype selectivity.[26] While additional inhibition of uptake could be observed at 500 nmol/rat,[26] the animals did not tolerate the higher dose. Brain uptake of no-carrier-added (*R,S*)-[^{18}F]-FMeQNB was inhibited by coinjection of 50 nmol/rat of the unlabeled antagonist (*R,S*)-FMeQNB but not with 50 nmol/rat of the M2 selective agonist, P-TZTP (3-[4-(propylthio)-1,2,5-thiadiazol-3-yl]-1,2,5,6-tetrahydro-1-methylpyridine)[32] (Fig. 1). The inhibition of uptake upon coinjection of unlabeled (*R,S*)-FMeQNB was especially significant in the heart, which contains 96% M2 subtype[33] (Table 1). The uptake of radioactivity was nearly uniform in all brain regions and the percentage inhibition was fairly uniform in all brain regions. The cerebellum showed proportionally higher inhibition of uptake due to the very high proportion of M2 subtype.

We also conducted displacement studies by injecting nonradiolabeled (*R,S*)-FMeQNB 60 min after injecting the labeled ligand. The tissue distribution was determined after an additional 60 min. Displacement was noted in the heart and some brain regions (Fig. 2a and Table 1) and indicated the reversibility of binding. This supports a receptor-based mechanism of ligand uptake and retention. The displacement is significant in the heart, and in those brain regions with the highest proportions of M2 subtype (pons, medulla, and cerebellum). Similar results were observed with administration of (*R*)-QNB 60 min after the radioligand (Fig. 2b and Table 1).

(*R,R*)-[^{18}F]-FMeQNB in rats

Similar uptake, coinjection, and displacement studies were conducted using the diastereomer (*R,R*)-[^{18}F]-FMeQNB. The uptake of (*R,R*)-[^{18}F]-FMeQNB (Fig. 3a) was more variable in brain tissues compared to the (*R,S*)-diastereomer. The uptake was higher in those tissues which contain a higher concentration of M1 subtype (cortex, hippocampus, and caudate) than in those which have a higher proportion of M2 sites (pons,

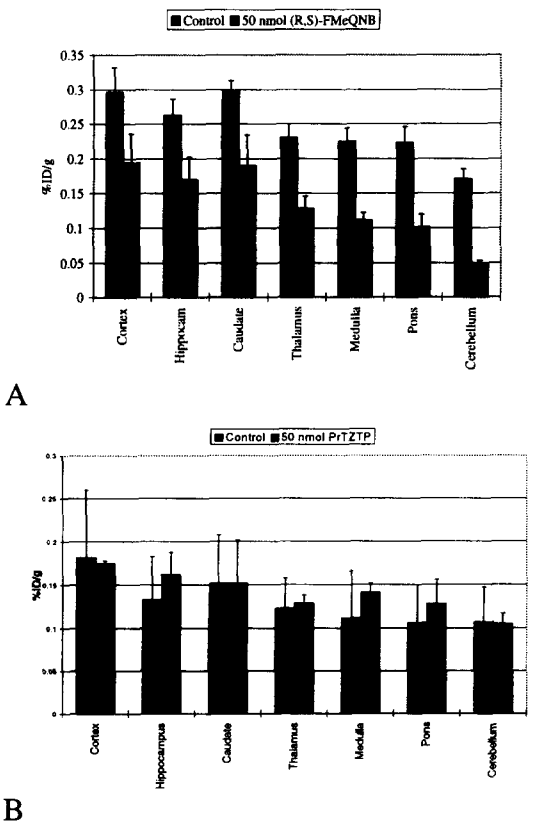

Figure 1. Coinjection of (*R,S*)-[^{18}F]-FMeQNB in rat brain with (A) nonradiolabeled (*R,S*)-FMeQNB (50 nmol) and (B) with nonradiolabeled P-TZTP (50 nmol). Sacrifice at 60 min. Data represent the mean of four to six rats. Error bars represent the standard deviation.

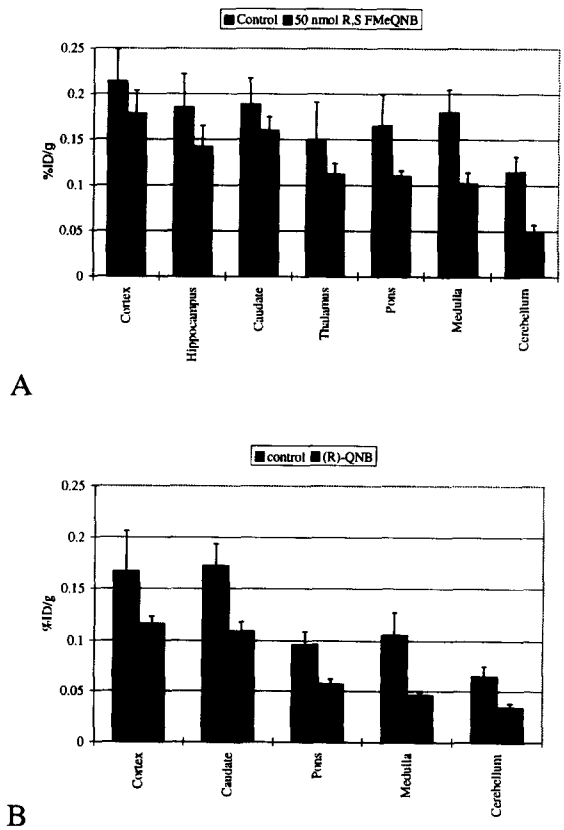

Figure 2. Displacement of (*R,S*)-[^{18}F]-FMeQNB in brain tissues with (A) (*R,S*)-FMeQNB (50 nmol) and (B) (*R*)-QNB (50 nmol) at 60 min. Sacrifice at 120 min. Data represent the mean of four to six rats per data point. Error bars represent the standard deviation.

Table 1. Percentage reduction of uptake upon coinjection and displacement in studies with (*R,S*)-[^{18}F]-FMeQNB[a]

Tissue	Coinjection with (*R,S*)-FMeQNB (%)	Displacement with (*R,S*)-FMeQNB (%)	Displacement with (*R*)-QNB (%)
Heart	92**	80**	74**
Cortex	34	16	30
Hippocampus	35*	23	ND
Caudate	36*	15	36
Thalamus	44**	24	ND
Pons	54**	33*	40*
Medulla	50**	43**	56*
Cerebellum	71**	57**	47*

[a]Percentage is defined as the percentage difference of the radiolabeled + nonradiolabeled compared to radiolabeled. An amount of 50 nmol of nonradiolabeled ligand per rat was administered. Significance was evaluated with single factor analysis of variance using Microsoft Excel. *$p < 0.01$, **$p < 0.001$, ND = tissue not collected.

medulla, and cerebellum). The uptake in the heart [0.3 or 0.7% ID/g ($n = 2$) at 60 min] was four to nine times lower than the uptake of the (*R,S*)-diastereomer (2.7% ID/g ($n = 2$) at 60 min). Inhibition of uptake upon coinjection of authentic (*R,R*)-FMeQNB (Fig. 3a and Table 2) was observed in all brain regions. However, the inhibition of uptake in pons, medulla, and cerebellum was not statistically significant due in part to the very low uptake and resulting poor counting statistics. Coinjection of (*R,S*)-FMeQNB (Fig. 3b and Table 2), which is M2 selective in vitro, showed significant uptake inhibition in thalamus, pons and heart.

A displacement study was conducted by administering 50 nmol of *R*-QNB 60 min after the radiolabel and sacrificing the animal after an additional 60 min (Fig. 4 and Table 2). Displacement of (*R,R*)-[^{18}F]-FMeQNB by (*R*)-QNB was significant in the cortex and in the hippocampus, tissues with a higher proportion of M1 relative to M2. This is consistent with higher M1 binding for (*R,R*)-[^{18}F]-FMeQNB.

Comparison of receptor selectivity

Subtype selectivity would require uptake of the ligand in all brain regions to follow the concentration of the corresponding subtype. An M2 specific ligand would display inhibition of uptake by coinjection or displacement in accordance with the concentration of muscarinic subtype. If nonspecific binding is negligible, an M2 selective ligand would display inhibition that is most pronounced in regions of the brain where the ratio of the concentration of M2 subtype to total muscarinic receptor is higher. Uptake and displacement in the heart provided a convincing argument for cardiac muscarinic selectivity of (*R,S*)-[^{18}F]-FMeQNB compared to its (*R,R*)-diastereomer. In the brain, M2 selectivity of (*R,S*)-[^{18}F]-FMeQNB was supported by the more uniform uptake of (*R,S*)-[^{18}F]-FMeQNB. (*R,R*)-[^{18}F]-FMeQNB shows lower uptake in those areas of the brain (pons, medulla, cerebellum) with a higher proportion of M2 subtype compared to those areas (cortex, hippocampus, thalamus) with higher M1 proportion. In addition, the displacement in the cerebellum suggested M2 selectivity for the (*R,S*)-diastereomer compared to the (*R,R*)-diastereomer because M2 receptors represent 88%[3] of cerebellar muscarinic receptors. However, in the other M2 rich brain regions, no statistical difference is noted.

(*R,R*)-[^{18}F]-FMeQNB shows higher uptake in cortex, hippocampus and caudate which are tissues with higher proportion of M1 binding sites. The heart uptake (0.3 or 0.7% ID/g at 60 min) is lower than that observed with the (*R,S*)-diastereomer (2.7% ID/g) and the uptake in the pons and medulla are lower. These data are

Table 2. Percentage reduction of uptake on coinjection and displacement in studies with (*R,R*)-[^{18}F]-FMeQNB[a]

Tissue	Coinjection with (*R,R*)-FMeQNB (%)	Coinjection with (*R,S*)-FMeQNB (%)	Displacement with *R*-QNB (%)
Heart	28*	60**	57*
Cortex	37*	21	53**
Hippocampus	45*	25	49*
Caudate	45*	20	12
Thalamus	43**	41**	20
Pons	47	41*	60*
Medulla	46	35	57*
Cerebellum	26	12	29

[a]Percentage is defined as the percentage difference of the radiolabeled + nonradiolabeled compared to radiolabeled. An amount of 50 nmol of nonradiolabeled ligand per rat was administered. Significance was evaluated with single factor analysis of variance using Microsoft Excel. *$p < 0.01$, **$p < 0.001$.

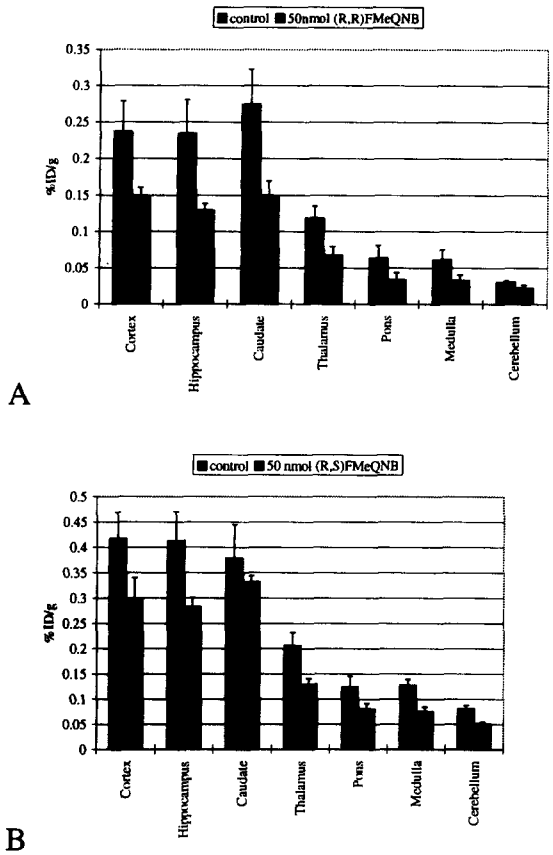

Figure 3. Coinjection of (*R,R*)-[^{18}F]-FMeQNB in brain with unlabeled (A) (*R,R*)-FMeQNB (50 nmol) and (B) (*R,S*)-FMeQNB (50 nmol) at 60 min. Data are the mean of four to six rats. Error bars represent the standard deviation.

consistent with M1 selectivity of (*R,R*)-[^{18}F]-FMeQNB. The tissues with higher M1 proportion also contain high M4 proportion. We did not measure M4 affinity for these compounds. We do have in vitro affinity of (*R*)-QNB at M4 in a cloned cell assay. The affinity at the various cloned subtypes for (*R*)-QNB were: M1 0.5, M2 0.3, M3 0.8, M4 0.4, M5 1.0 nM. We would expect the

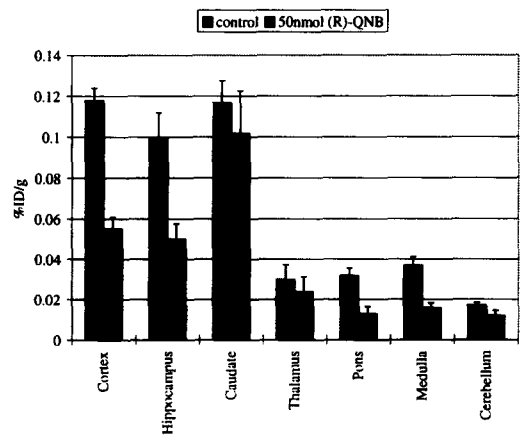

Figure 4. Displacement of (*R,R*)-[^{18}F]-FMeQNB in brain with (*R*)-QNB at 60 min (50 nmol). Sacrifice at 120 min. Data are the mean of four to six rats per point. Error bars represent the standard deviation.

FMeQNB diastereomers to have M4 affinity within the same range and therefore M4 binding may be a component of the tissue distribution. Thus we must propose combined M1 and M4 (M1/M4) binding.

The displacement studies with (*R*)-QNB did not provide the clear distinction we had expected. Since (*R*)-QNB is M2 selective in vivo, we would expect more displacement of the (*R,R*)-[^{18}F]-FMeQNB bound to the M2 receptor subtype than to the M1/M4 subtype. The pons and medulla showed high displacement but displacement in the cerebellum was not statistically significant. Significant displacement was observed in cortex and hippocampus where one would expect M1 uptake to be the major process. Lee et al. addressed these same types of discrepancies and showed that uptake inhibition observed on coinjection of 50 nmol of nonradiolabeled ligand correlated not with the affinity of the various ligands but with the RBI (relative binding index, the ratio of the affinity of the test compound and the affinity for the radiolabeled compound, [^{125}I]-IQNB).[26]

Monkeys

Because we are ultimately interested in studying muscarinic receptors in the human brain and in human diseases, we needed to know if the results observed in rats can translate to primates and ultimately to humans. Therefore, we performed PET studies in rhesus monkey. (*R,S*)-[^{18}F]-FMeQNB exhibited prolonged uptake and retention over 5 h. The uptake in cortical regions continued to increase but clearance was observed from the cerebellum (Fig. 5a). Attempts to displace the radiolabel with a dose of nonradiolabeled (*R,S*)-FMeQNB 60 min following injection of the radiolabeled compound were unsuccessful. This is probably due to the slow receptor off-rate of the radiolabeled ligand combined with the instability in blood of unlabeled (*R,S*)-FMeQNB. Use of (*R*)-QNB as the unlabeled displacer and observing for 5 h resulted in evidence of displacement (Fig. 5b). The displacement in tissue regions was determined in the following way. The change in activity between predisplacement (40–60 min) and postdisplacement (270–300 min) was calculated. Two displacement experiments were compared with one control study to determine the percent displacement. Displacement from thalamus, cortical regions, basal ganglia, and cerebellum were 50%, 35–38%, 26%, and 14%, respectively. The relatively higher percent displacement from the thalamus which has higher proportion of M2 subtype compared to cortical regions[2] is again consistent with M2 selectivity. However, the displacement from the cerebellum, which is predominantly M2, was unexplainably low.

Interpretation of uptake and clearance kinetics and the resultant modeling of receptor kinetics requires a reliable estimate of the blood concentration of the ligand as a function of time. Periodically during the course of the scanning, arterial blood samples are

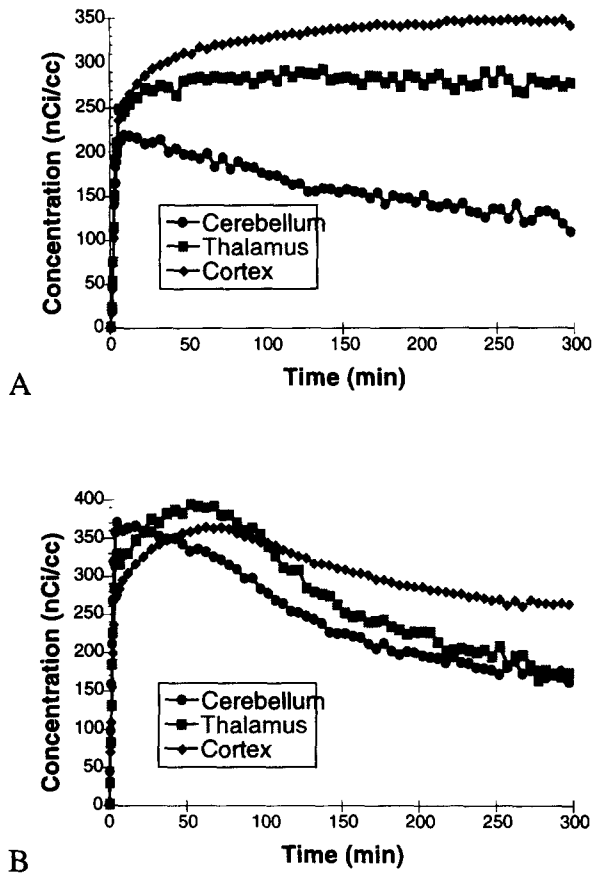

Figure 5. Tissue activity curve of (*R*,*S*)-[^{18}F]-FMeQNB (2.3 mCi) in monkey. (A) Control study; (B) displacement with (*R*)-QNB (67 μg/kg at 60 min).

analyzed for radioactive components in the plasma. Generally, we utilize the in vitro blood metabolite assay to estimate the concentration of parent radioligand at the time of injection. This assay uses blood drawn from the animal prior to the start of the scanning session. The

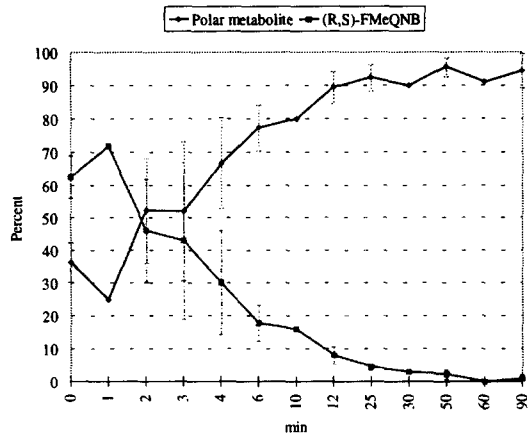

Figure 6. Radiolabeled components in monkey plasma after injection of (*R*,*S*)-[^{18}F]-FMeQNB. Errors bars represent the standard deviation. Where no error bar is present, $n = 1$; otherwise, $n = 3$ or 4.

blood is spiked with some of the injected radioligand and processed as a normal metabolite assay. However, because of the instability in blood discussed earlier, this assay may not be reliable. Consequently, the plasma concentration of parent compound at time of injection was extrapolated from the later time points.

After bolus administration of (*R*,*S*)-[^{18}F]-FMeQNB, the radioligand was metabolized rapidly. The measured parent and metabolite fractions are shown in Fig. 6. The free fraction in plasma was measured at 11%. A large amount of the radioactivity in the plasma was determined to be a polar metabolite, probably fluoride, based on bone uptake as visualized in the skeleton at late time points. The parent represented less than 5% of the extractable blood activity at 30 min postinjection.

In one study, the monkey was repositioned to observe the myocardial uptake at 30–40 min (Fig. 7). Good contrast between myocardium and blood pool was

Figure 7. (*R*,*S*)-[^{18}F]-FMeQNB in the myocardium of a rhesus monkey. Two adjacent slices acquired 30–40 min after bolus injection of 1.6 mCi. Maximum activity in the myocardium is ~700 nCi/cm^3. The bright spot at upper right is probably bone uptake.

observed consistent with M2 selective uptake and retention. Thus (*R,S*)-FMeQNB has potential for imaging cardiac muscarinic receptors.

Conclusions

(*R,S*)-[^{18}F]-FMeQNB displayed uptake and displacement properties consistent with a M2 selective ligand in both rats and monkeys. Uptake could be inhibited by coinjection of QNB analogues but not with the muscarinic agonist, P-TZTP. In rats, the uptake was similar in all of the brain regions and the reduction of uptake by coinjecting nonradiolabeled ligand was nearly uniform. Uptake into the heart was extremely high and inhibition of uptake upon coinjection or displacement by nonradiolabeled ligand is very significant. Displacement by nonradiolabeled ligand or by (*R*)-QNB was significant only in the M2-rich regions—pons, medulla, and cerebellum. In monkeys, (*R,S*)-[^{18}F]-FMeQNB was taken up into the brain and exhibits very slow clearance. The thalamus contains a higher concentration of M2 subtype than the cerebellum and a higher proportion of M2 subtype when compared to the cortex. Displacement proceeded to a greater extent in the thalamus than in the cortex (Fig. 5b). Displacement by *R*-QNB from the monkey cerebellum was modest; however this result may explained by the low concentration of M2 subtype.

On the other hand, its diastereomer, (*R,R*)-[^{18}F]-FMeQNB, displayed uptake better explained by M1/M4 selectivity. First, it displayed significantly lower uptake into the rat heart. Second, there was higher uptake into those brain regions with a higher proportion of M1/M4 subtypes (cortex, hippocampus, caudate) than in those brain regions with higher M2 proportions. The uptake inhibition by coinjection and displacement data for (*R,R*)-[^{18}F]-FMeQNB were not as easily explained in terms of M1/M4 versus M2 selectivity presumably due to the kinetic differences at these receptor subtypes.

These radioligands do display differential subtype selectivity and may prove useful for the in vivo imaging of muscarinic receptor subtypes. However, the apparently very low off-rate of binding and rapid metabolism may limit the ability to determine the kinetic parameters necessary to evaluate the change in receptor concentration as a function of disease.

Experimental

General

Thin-layer chromatography (TLC) analyses used Whatman LK6DF plates eluted with $CHCl_3$/MeOH/NH_4OH (90:9:1). Flash chromatography utilized home-made columns, Macherey–Nagel 230–400 mesh silica gel, a 6-in column height, and the column diameter specified in the experimental. ^{1}H and ^{13}C NMR spectra were obtained from a Varian VXR-200 at 200 or 50.3 MHz, respectively, and were taken in chloroform unless otherwise stated. Radioactivity was quantitated using either a Bioscan System 200 Imaging Scanner or a Fuji BAS-1500 Phosphorimager.

Chemical synthesis

Authentic (*R,S*)-FMeQNB, (*R,R*)-FMeQNB, and (1*R*,2*S*,5*R*)-5-methyl-2-(1-methyl-1-phenylethyl)cyclohexyl-(*S*)-α-hydroxy-α-(4-[hydroxymethyl]-phenyl)benzeneacetate (**1**) [8-phenylmenthyl-(*S*)-hydroxymethyl benzilate] were prepared as described.[23]

(*S*)-α-Hydroxy-α-(4-hydroxymethyl)phenyl benzeneacetic acid (2). 8-Phenylmenthyl-(*S*)-hydroxymethyl benzilic acid (**1**) (1.3 g, 2.75 mmol) was dissolved in 30 mL ethanol and 6 mL water. KOH (3.37 mL of 45% aqueous, 27 mmol) was added and the resultant solution heated at 85 °C for 2.5 h. The solvent was concentrated and the residue taken up in 1 N NaOH (25 mL). The mixture was extracted with CH_2Cl_2 (2 × 25 mL). The aqueous portion was acidified with HCl and the resultant mixture extracted with CH_2Cl_2:EtOAc (1:1) (2 × 25 mL). The extracts were dried (Na_2SO_4) and evaporated. The product was crystallized from ethyl acetate/hexane to give the solid acid (405 mg, 60%): ^{1}H NMR ($CDCl_3$/DMSO-d_6) δ 7.55–7.40 (m, 4H), 7.40–7.25 (m, 5H), 5.22 (brs, 1H), 4.60 (s, 2H); ^{13}C NMR ($CDCl_3$/DMSO-d_6) δ 175.1, 142.2, 140.8, 140.8, 127.0, 126.8, 126.6, 126.6, 125.5, 79.7, 63.1; anal. calcd for $C_{15}H_{14}O_4$: C, 69.74%; H, 5.47%. Found C, 69.80%; H, 5.48%.

4-Methylbenzoylformic acid. Ethyl 4-methylbenzoylformate (6.55 g, 34.11 mmol) was suspended in 20.5 mL 2 N NaOH and stirred overnight. The resulting solution was diluted with 30 mL H_2O and extracted with $CHCl_3$ (2 × 20 mL). The aqueous layer was acidified with concentrated HCl and extracted with $CHCl_3$ (2 × 20 mL). The organic layers were dried (Na_2SO_4) and evaporated to give 5.2 g (95%) of the acid. This material was used directly in the next step without any additional purification: ^{1}H NMR δ 10.125 s, 8.14 (d, J = 8 Hz, 2H), 7.30 (d, J = 8 Hz, 2H), 2.44 (s, 3H); ^{13}CNMR δ 187.8, 167.07, 150.52, 134.53, 133.08, 132.67, 25.31.

8-Phenylmenthyl 4-methylbenzoylformate (7). 4-Methylbenzoylformic acid (1.58 g, 9.63 mmol) was first treated with α,α-dichloromethyl methyl ether (860 μL, 9.5 mmol) for 1 h at 65 °C. The solution was removed from the heating bath, diluted with 10 mL CH_2Cl_2, and added dropwise to an ice-cooled solution of 8-phenylmenthol (2 g, 8.62 mmol) and triethylamine (1.57 mL, 11.2 mmol) in CH_2Cl_2 (20 mL). The resultant solution was allowed to warm to room temperature and stirred overnight. The solution was washed with water, dried (Na_2SO_4), and evaporated. The residue was subjected to flash chromatography (50 mm column, 10% EtOAc in hexane) to give 1.76 g (54%) of the product as a colorless, viscous oil: ^{1}H NMR δ 7.86 (d, J = 8 Hz, 2H), 7.3–6.9 (m, 7H), 5.01 (dt, J = 11, 5 Hz, 1H), 2.4 (s, 3H),

2.1–1.9 (m, 2H), 1.7–1.4 (m, 3H), 1.35 (s, 3H), 1.31 (s, 3H), 1.28–0.96 (m, 3H), 0.90 (d, J = 6 Hz, 3H); ^{13}C NMR δ 185.46, 162.98, 150.25, 145.804, 130.21, 129.45, 127.98, 125.51, 125.29, 77.39, 50.57, 41.41, 40.05, 34.38, 31.46, 27.82, 26.97, 25.85.

8-Phenylmenthyl-(*R*)-4-methylbenzilate. 8-Phenylmenthyl benzoylformate (1.76 g, 4.66 mmol) was dissolved in 10 mL THF and cooled in dry ice/acetone bath. Phenyl magnesium bromide (1.7 mL of 3 M) was added dropwise over a few minutes. The reaction was allowed to stir and warm to room temperature overnight. The solution was poured into 10% NH_4Cl and extracted with $CHCl_3$ (2 × 80 mL). The organic layers were dried (Na_2SO_4) and evaporated. The crude product (2.3 g, 108%) from this reaction was examined by ^{1}H NMR and was deemed pure enough to be used directly for the next step. In other preparations it was necessary to purify the material by flash chromatography (10% EtOAc in hexane). NMR and mass spectral data were obtained from a preparation which had been purified by chromatography: ^{1}H NMR δ 7.52–7.40 (m, 2H), 7.39–7.28 (m, 3H), 7.28–7.13 (m, 2H), 7.13–6.98 (m, 7H), 4.86 (dt, J = 6, 4 Hz, 1H), 2.79 (s, 1H), 2.27 (s, 3H), 2.19–1.88 (m, 3H), 1.71–1.33 (m, 4H), 1.086 (s, 3H), 1.013 (s, 3H), 0.845 (d, J = 5 Hz, 3H); ^{13}C NMR δ 172.15, 151.22, 142.11, 139.26, 137.44, 128.61, 128.12, 127.90, 127.83, 127.33, 127.07, 127.07, 125.28, 125.20, 80.80, 78.11, 50.11, 40.97, 39.57, 34.49, 31.37, 27.17, 26.85, 25.60, 21.71, 21.01; EIMS 456 (very small), 197 (100), 105 (100); CIMS (NH_3) 474 (M+18).

8-Phenylmenthyl-4-(bromomethyl)benzilate. 8-Phenylmenthyl 4-methylbenzilate (2.12 g, 4.65 mmol) was dissolved in CCl_4 (90 mL) and treated with *N*-bromosuccinimide (827 mg, 4.65 mmol) and a catalytic amount of benzoyl peroxide (10 mg) at reflux for 2 h and then while still at reflux under an intense lamp for 2 h. The insoluble low-density succinimide was removed by filtration. The solvent was evaporated and the residue subjected to flash chromatography (50 mm, 10% EtOAc/hexane). The separation provided a product contaminated with minor amounts of a substituted benzophenone and dibromination (^{1}H NMR δ 6.6 singlet). The monobromo product predominates and shows a singlet in the ^{1}H NMR at δ 4.35 (1.77 g, 70%). This impure material was carried on directly to the next step.

(1*R*,2*S*,5*R*)-5-Methyl-2-(1-methyl-1-phenylethyl)-cyclohexyl-(*R*)-α-hydroxy-α-(4-[hydroxymethyl]-phenyl) benzeneacetate (8). The crude 4-bromomethyl benzilate (1.53 g, 2.86 mmol) was suspended in 15 mL CH_3CN. The solution was treated with AgOTFA (11.27 g, 5.73 mmol) and stirred overnight. The mixture was filtered and evaporated. The residue was taken up in 15 mL ethanol and treated with 2 mL 0.1 M NaOH for 1 h then 1 mL 1 N NaOH was added and the mixture stirred for 2 h. Finally a third portion of 1 mL of 1 N NaOH was added and stirring continued for 2 h more. Water was added (80 mL) and the mixture extracted with $CHCl_3$ (2 × 40 mL). The combined organic layers were dried (Na_2SO_4) and evaporated. The residue was subjected to flash chromatography (50 mm, 30% EtOAc/hexane) to provide the desired product 890 mg (66%) and a side product (175 mg) identified as the aldehyde (^{1}H NMR δ 9.9 singlet) derived from hydrolysis of the dibromo impurity.

HPLC analysis (Axxiom C-18; 4.6 mm × 250 mm, 65% CH_3CN/35% water, 2 mL/min) showed the diastereomeric purity to be 97%. Elution time 14.4 min for major isomer, 13.6 min for minor isomer: ^{1}H NMR δ 7.49–7.18 (m, 9H), 7.08 (brs, 5H), 4.86 (dt, J = 6, 4 Hz, 1H), 4.6 (brs, 2H), 2.74 (brs, 1H), 2.21–1.88 (m,3H), 1.76–1.55 (m, 2H), 1.15–1.04 (m, 2H) 1.08 (s, 3H), 1.01 (s, 3H), 0.85 (d, J = 6 Hz, 3H); ^{13}C NMR δ 171.87, 151.24, 141.90, 141.57, 140.386, 128.13, 127.97, 127.40 127.27, 126.47, 125.23, 80.78, 78.18, 64.94, 50.06, 40.97, 39.53, 34.48, 31.36, 27.44, 26.81, 25.31, 25.27, 21.70; CIMS (NH_3) 490 (M + 18); HREIMS calcd for $C_{31}H_{36}O_4$ 472.2513; obsd 472.2595.

(*R*)-α-(4-[Hydroxymethyl]-phenyl benzeneacetic acid (9). The 4-hydroxymethyl analogue (**8**) (860 mg, 1.8 mmol) was dissolved in 20 mL ethanol and 4 mL water. KOH (2.25 mL of 45% aqueous, 18 mmol) was added and the reaction heated at 80 °C for 2 h. The ethanol was evaporated, the residue treated with 1 N NaOH (20 mL) and extracted with one portion of CH_2Cl_2. The aqueous portion was acidified with concentrated HCl and the mixture extracted with 2 × 25 mL portions of 1:1 ethylacetate:CH_2Cl_2. The organic layer was dried and evaporated. The residue was crystallized from EtOAc/hexane to give 233 mg (55%): ^{1}H NMR ($CDCl_3$, DMSO-d_6) δ 7.50–7.31 (m, 4H), 7.31–7.08 (m, 5H), 4.94 (s, 1H), 4.54 (s, 2H); ^{13}C NMR ($CDCl_3$, DMSO-d_6) δ 175.8, 142.7, 141.5, 141.4, 127.7, 127.5, 127.3, 126.3, 80.3, 63.9; anal. calcd for $C_{15}H_{14}O_4$: C, 69.74%; H, 5.47%; found C, 69.95%; H, 5.54%.

Piperonyl (*S*)-α-(4-[methanesulfonyloxymethyl]-phenyl benzeneacetate (4). (*S*)-Hydroxymethyl benzilic acid (**2**) (217 mg, 0.896 mmol), Et_3N (125 μL, 0.90 mmol), and piperonyl chloride (152 mg, 0.894 mmol) were dissolved in 200 μL DMF. The mixture was stirred overnight. Water (10 mL) and $CHCl_3$ (10 mL) were added and the organic layer separated, dried over Na_2SO_4, and evaporated. The residue was subjected to flash chromatography (30 mm diameter, 45% EtOAc/hexane) to give 144 mg (41%) of product as a foam: ^{1}H NMR δ 7.42–7.15 m, 6.72 s, 6.59 s, 5.90 s, 5.15 s, 4.60 s, 4.33 s.

The piperonyl ester (**3**) (144 mg, 0.367 mmol) was dissolved in 4 mL CH_2Cl_2. Et_3N (56 μL, 0.404 mmol) and methanesulfonyl chloride (32 μL, 0.404 mmol) were added. The solution was stirred for 2.5 h. An additional 14 μL (0.18 mmol) methanesulfonyl chloride and 27 μL (0.19 mmol) Et_3N were added and the reaction stirred an additional hour. The reaction solution was evaporated and subjected to flash chromatography (30 mm diameter, 40% EtOAc/hexane) to give the product as an oil (134 mg, 77%). The mesylate was used as a precursor for labeling without any additional purifica-

tion: ^{1}H NMR δ 7.5–7.40 (m, 2H), 7.39–7.22 (m, 5H), 6.75 (s, 2H), 6.67 (s, 1H), 5.95 (s, 2H), 5.22 (s, 2H), 5.18 (s, 2H), 4.34 (s, 1H), 2.90 (s, 3H); ^{13}C NMR 173.7, 147.8, 147.4, 142.9, 141.5, 133.0, 128.3, 128.2, 128.1, 127.9, 127.1, 12.3, 108.8, 108.1, 101.1, 80.7, 70.8, 68.4, 38.1.

Piperonyl (*R*)-α-(4-[methanesulfonyloxymethyl]-phenyl benzeneacetate. A solution of (*R*)-hydroxymethyl benzilic acid (**9**) (220 mg, 0.852 mmol), piperonyl chloride (152 mg), and Et_3N (118 μL) was stirred overnight. The solution was warmed in a 60 °C oil bath for 10 min, cooled to room temperature, then was treated with 10 mL water and 10 mL $CHCl_3$. The layers were separated and the aqueous portion extracted with a second 10 mL portion of $CHCl_3$. The organic layers were dried over Na_2SO_4 and evaporated. The residue was subjected to flash chromatography (20 mm, 45% EtOAc, 55% hexane) to yield the product (197 mg, 59%). The alcohol was used without additional purification: ^{1}H NMR δ 7.43–7.16 (m, 9H), 6.70 (s, 2H), 6.59 (s, 1H), 5.90 (s, 2H), 5.13 (s, 2H), 4.60 (s, 2H), 4.30 (s, 1H); ^{13}C NMR 174.0, 147.7, 147.8, 141.7, 141.1, 140.7, 128.4, 128.0, 127.6, 127.3, 126.5, 122.2, 108.8, 108.1, 101.1, 80.9, 68.3, 64.7, 29.6.

The alcohol (197 mg, 0.502 mmol) was dissolved in 5 mL CH_2CL_2. Et_3N (84 μL, 0.603 mmol) and methanesulfonyl chloride (46 μL, 0.603 mmol) were added. After 1 h an additional 5 μL (0.1 mmol) methanesulfonyl chloride was added. After an additional 20 min the reaction was partitioned with 5 mL water. The organic layer was dried and evaporated. The residue was subjected to flash chromatography (30 mm diameter, 40% EtOAc in hexane) to give 144 mg (61%) as an oil. The mesylate was used as labeling precursor without any additional purification: ^{1}H NMR δ 7.5–7.22 (m, 9H), 6.72 (s, 2H), 6.64 (s, 1H), 5.93 (s, 2H), 5.21 (s, 2H), 5.16 (s, 2H), 3.97 (brs, 1H), 2.90 (s, 3H); ^{13}C NMR δ 173.7, 147.8, 147.7, 172.9, 141.5, 133.1, 128.3, 128.0, 127.1, 122.4, 108.8, 101.2, 80.7, 70.8, 68.5, 38.2.

Radiochemical synthesis

A 13 mm × 100 mm test tube was charged with Kryptofix 2.2.2 (50 μL of CH_3CN containing 2.25 mg, 6.0 μmol) and K_2CO_3 (30 μL, 0.1 M in water, 3 μmol). [^{18}F]-Fluoride in water (up to 400 μL containing as much as 73 mCi) was added and the solution evaporated to dryness with an argon stream while heating in a 100 °C heating block. Three 200 μL portions of acetonitrile were added and evaporation was conducted after each portion in order to azeotropically remove residual water. Piperonyl (*S*)-α-(4-[methanesulfonyloxymethyl]-phenyl benzeneacetate (**4**) (or the (*R*) enantiomer) (3.38 mg, 7.2 μmol) in 200 μL CH_3CN was then added. The resulting mixture was heated at 100 °C for 5 min. The mixture was cooled in a water bath briefly then transferred to a short column of silica gel (about 7 mm) in a pasteur pipet. The reaction tube was rinsed with 1 mL of CH_2Cl_2 and the solvent added to the column. The liquid was pushed through the column with air pressure generated by a pipet bulb and then the column was eluted with an additional 1 mL of CH_2Cl_2.

The eluate was evaporated to dryness under an argon stream while placed in a 60 °C heating block. When dry, the tube was placed into a room temperature water bath and trifluoroacetic acid (100 μL) was added. The reaction was allowed to stand for 2 min. The acid was blown off with an argon stream in the 60 °C heating block. When dry, a solution of carbonyl diimidazole (8.1 mg, 50 μmol) in 50 μL DMF was added, the reaction vortexed and then placed into a 100 °C heating block for 2 min. Then a solution of (*R*)-quinuclidinol (9 mg, 71 μmol) in 100 μL DMF was added. The solution was heated for another 5 min and then placed into a cool-water bath.

HPLC eluant (see below) (500 μL) was added and the resulting mixture filtered through a 13 mm MILLEX-GV filter. The reaction tube and filter were rinsed with an additional 200 μL of eluant. The filtrate was injected onto a Beckman C-18 column (9.5 mm × 250 mm) and eluted with 40% CH_3CN and 60% buffer (5 mM NaH_2PO_4, 5 mM Et_3N, pH adjusted to 6.8 with H_3PO_4) at 7 mL/min. The product eluted at approximately 17–18 min in a volume of 10–12 mL.

A BondElut C-18 was rinsed with 0.5 mL 5% K_2CO_3, 2 mL ether, 2 mL ethanol, and 4 mL water. The product-containing eluate from the HPLC was treated with 0.5 mL of 5% K_2CO_3 prior to passing through the BondElut C-18 to retain the product. The column was rinsed with 2 mL water. Elution of the product from the BondElut C-18 was accomplished with 2 mL of 25% ethanol in ether. The radiochemical yield was calculated from the activity collected at this point. The eluate was evaporated with a stream of argon while being warmed at 60 °C.

Formulation of the product was achieved by taking an aliquot containing the required activity, diluting to 9 mL with normal saline and filtering through a 13 mm MILLEX-GV sterile filter into a sterile vial.

Specific activity was determined from an aliquot prior to formulation. If required, the aliquot was concentrated under an argon stream at room temperature. The product was then injected on an Axxiom C-18 HPLC column (4.6 mm × 250 mm) and eluted with 65% CH_3CN and 35% buffer (5 mM NaH_2PO_4, 5 mM Et_3N) at 1.5 mL/min. The product eluted at about 10 min. The UV was monitored at 230 nm and the mass was determined by comparing to a standard curve for the authentic product. Identity has been shown by coinjection of authentic product with the radioactive product and observing coelution.

Plasma protein binding

A sample (300 μL) of plasma was filtered through an anisotropic, hydrophilic YMT ultrafiltration membrane (Centrifree Micropartition System, Product No. 4104, Amicon, Inc.). An aliquot (100 μL) of this protein-free filtrate was counted on a gamma counter as well as 100 μL of plasma. The counts were decay corrected to the same time and the free fraction was determined by the ratio of the counts of the protein free filtrate to the counts of the plasma. Each determination was done in duplicate.

In vivo biodistribution in rats

For coinjection studies, rats were injected with 30 μCi of ^{18}F radioligand or coinjected with 30 μCi of ^{18}F radioligand and 50 nmol of nonradiolabeled ligand. For displacement studies, rats were injected with 30 μCi of ^{18}F radioligand only or 30 μCi of ^{18}F radioligand followed 60 min later by of 50 nmol of nonradiolabeled ligand. The rats were sacrificed at 60 min following the last injection (radiolabel or postinjection) and the brain immediately placed in 0.3 M sucrose on ice. The brain was dissected on ice. Blood and various tissue samples were taken from each animal, weighed, and radioactive content assessed by gamma counting. The percent injected dose per gram (% ID/g) was determined. All data are expressed as means of three to six rats.

In vitro stability studies.Saline and phosphate buffers

[^{18}F]-FMeQNB (50 μL, 50 μCi) was added to 1 mL of each of the following: saline, saline with 5 mM NaH_2PO_4, water, 5 mM NaH_2PO_4, and 50 mM NaH_2PO_4 (measured pH 5) and allowed to stand at room temperature. Aliquots for TLC were spotted directly from the solutions at 0, 60, and 120 min (except for 50 mM NaH_2PO_4). The 50 mM NaH_2PO_4 caused the TLC spots to streak unless the eluant was made fresh each time.

Metabolite analysis

The blood sample was centrifuged to separate the plasma and the red cells. A portion (300 μL) of the plasma was mixed with 300 μL acetonitrile and vortexed; the resultant mixture was centrifuged for 3 min. The supernatant and pellet were counted to determine percent recovery. A 100 μL aliquot of the supernatant was concentrated under a stream of argon prior to spotting on Whatman LK6DF silica gel plates. The plates were developed with $CHCl_3$:MeOH:NH_4OH (90:9:1). Following development the radioactivity was counted using either a Bioscan System 200 Imaging Scanner or a Fuji BAS-1500 Phosphoimager to determine the percentage parent extracted into the aqueous acetonitrile.

Plasma stability

Plasma was separated by centrifugation from monkey blood and cooled on ice. [^{18}F]-FMeQNB (20 μL, 22 μCi) was added to 300 μL of iced plasma; the plasma was allowed to stand at room temperature during the duration of the experiment. After set times of 0, 10, 30, 60 min, 50 μL of the plasma was removed and treated with 50 μL CH_3CN to precipate proteins. The solid was separated by centrifugation and the supernatant assayed by TLC (see the metabolite assay) to determine the percentage parent.

Effects of anesthetics

Blood was obtained from rhesus monkey and rat. The monkey blood was obtained under the following protocol and stored on ice: (1) inject with 0.8 mL ketamine (10 mg/kg) im and after 20 min obtain 4 mL arterial blood; (2) inject with 0.5 mL atropine (0.03 mg/kg) im and after an additional 10 min obtain 4 mL arterial blood; (3) inject with 2 mL 2.5% pentothal iv and after 10 min obtain 4 mL arterial blood.

The rat blood was obtained under a similar anesthetic protocol: (1) inject with ketamine (100 mg/kg) im, sacrifice at 10 min to collect blood by cardiac puncture; (2) inject with ketamine im, atropine (0.4 mg/kg) im, then pentothal (0.15 mL of 2.5%) iv, sacrifice at 10 min to collect blood by cardiac puncture.

Each sample was spiked with 5 μL of a stock solution of [^{18}F]-FMeQNB and worked up as described for metabolite assay. Plasma protein binding was also determined.

Temperature stability study

Rhesus monkey blood was divided into two 2 mL portions and stored on ice for 2–3 h prior to use. One sample of blood and 2 mL of saline were set into a 37 °C water bath for 10 min. The second sample and another sample of saline remained in ice for 10 min. Then each sample was treated with a 40 μL aliquot of [^{18}F]-FMeQNB in ethanol. After a short time, the blood samples were returned to ice, and metabolite analysis was performed.

PET imaging studies

PET studies were performed in rhesus monkeys ($\sim$10 kg). Animals were initially anesthetized with ketamine. Endotracheal intubation was performed for control of respiration and an intravenous line was inserted in a distal lower extremity. Arterial sampling was performed with an indwelling port. The animals were transported to the PET suite, placed under isoflurane anesthesia, and positioned on the scanning table. Blood pressure, EKG, temperature, and end-tidal pCO_2 were continuously monitored. The head was positioned in a

stereotactic head holder so that scans were acquired in the coronal plane. All studies were performed under a protocol approved by the NIH Clinical Center Animal Care and Use Committee.

Scans were performed with the GE Advance tomograph[34] which acquires 35 simultaneous slices, with a 4.25 mm inter-slice distance. Scans were acquired in three-dimensional mode with septa removed producing a reconstructed resolution of 6 mm in all directions. Transmission scans were acquired with two rotating rod sources. Image reconstruction included corrections for attenuation, scatter, randoms, and deadtime. Pixel values were calibrated in nCi/mL with a uniform phantom filled with ^{18}F.

Following transmission scans, three to five injections of 4 mCi of [^{15}O]-water were performed with a 3 min scan acquired beginning 10 s after each injection. Images from these studies were averaged and used for placement of regions of interest. (*R,S*)-[^{18}F]-FMeQNB studies were performed with bolus administration of ~1–2 mCi, administered iv over a 10-min period. Dynamic scans were acquired beginning with tracer injection for a period of at least 90 min. Postinjections were administered iv at the appropriate time. Serial arterial blood samples were collected for up to 5 h. Samples were centrifuged and a 0.1 mL portion counted in a calibrated gamma counter. Five to eight samples were analyzed for metabolite fraction by TLC using the procedure described in the metabolite analysis section.

Acknowledgements

P-TZTP was a generous gift from Novo Nordisk. The authors acknowledge Susan Fluck, Wendy Sandoval, and Dr John Bacher for invaluable assistance with primate studies, Debra Drumm for assistance with rat studies, and the cyclotron staff for isotope production.

We gratefully acknowledge the NIMH/NOVASCREEN® Psychotherapeutic Drug Discovery and Development Program (Contract No. N01MH20003) for in vitro receptor binding assays.

References

1. Levey, A. I. *Life Sci.* **1993**, *52*, 441.

2. Flynn, D. D.; Mash, D. C. *Synapse* **1993**, *14*, 283.

3. Gitler, M. S.; Cohen, V. I.; de la Cruz, R.; Boulay, S. F.; Jin, B.; Zeeberg, B. R.; Reba, R. C. *Life Sci.* **1993**, *53*, 1743.

4. Quirion, R.; Aubert, I.; Lapchak, P. A.; Schaum, R. P.; Teolis, S.; Gauthier, S.; Araujo, D. M. *Trends in Pharmacol. Sci.* **1989**, 80.

5. Aubert, I.; Araujo, D. M.; Cecyre, D.; Robitaille, Y.; Gauthier, S.; Quirion, R. *J. Neurochem.* **1992**, *58*, 529.

6. Flynn, D. D.; Ferrari-DiLeo, G.; Mash, D. C.; Levey, A. I. *J. Neurochem.* **1995**, *64*, 1888.

7. Maziere, M. *Pharmac. Ther.* **1995**, *66*, 83.

8. Tavitian, B.; Pappata, S.; Bonnot-Lours, S.; Prenant, C.; Jobert, A.; Crouzel, C. *Eur. J. Pharmacol.* **1993**, *236*, 229.

9. Dewey, S. L.; MacGregor, R. R.; Brodie, J. D.; Bendriem, B.; King, P. T.; Volkow, N. D.; Schlyer, D. J.; Fowler, J. S.; Wolf, A. P.; Gatley, S. J.; Hitzemann, R. *Synapse* **1990**, *5*, 213.

10. Dannals, R. F.; Langstrom, B.; Ravert, H. T.; Wilson, A. A.; Wagner, Jr. H. N. *Appl. Radiat. Isotop* **1988**, *39*, 291.

11. Varastet, M.; Brouillet, E.; Chavoix, C.; Prenant, C.; Crouzel, C.; Stulzaft, O.; Bottlaender, M.; Cayla, J.; Maziere, B.; Maziere, M. *Eur. J. Pharmacol.* **1992**, *213*, 275.

12. Frey, K. A.; Koeppe, R. A.; Mulholland, G. K.; Jewett, D.; Hichwa, R.; Ehrenkaufer, R. L. E.; Carey, J. E.; Wieland, D. M.; Kuhl, D. E.; Agranoff, B. W. *J. Cereb. Blood Flow Metab.* **1992**, *12*, 147.

13. Koeppe, R. A.; Frey, K. A.; Mulholland, G. K.; Kilbourn, M. R.; Buck, A.; Lee, K. S.; Kuhl, D. E. *J. Cereb. Blood Flow Metab.* **1994**, *14*, 85.

14. Hwang, D. R.; Dence, C. S.; McKinnon, Z. A.; Mathias, C. J.; Welch, M. J. *Nucl. Med. Biol.* **1991**, *18*, 247.

15. Farde, L.; Suhara, T.; Halldin, C.; Nyback, H.; Nakashima, Y.; Swahn, C.-G.; Karlsson, P.; Ginovart, N.; Bymaster, F. P.; Shannon, H. E.; Foged, C.; Suzdak, P. D.; Sauerberg, P. *Dementia* **1996**, *7*, 187.

16. Gitler, M. S.; Boulay, S. F.; Sood, V. K.; McPherson, D. W.; Knapp, Jr. F. F.; Zeeberg, B. R.; Reba, R. C. *Brain Research* **1995**, *687*, 71.

17. McPherson, D. W.; Lambert, C. R.; Jahn, K.; Sood, V.; McRee, R. C.; Zeeberg, B.; Reba, R. C.; Knapp, F. F. *J. Med. Chem.* **1995**, *38*, 3908.

18. McPherson, D. W.; DeHaven-Hudkins, D. L.; Callahan, A. P.; Knapp, F. F. *J. Med. Chem.* **1993**, *36*, 848.

19. Gibson, R. E.; Moody, T.; Schneidau, T. A.; Jagoda, E. M.; Reba, R. C. *Life•Sci.* **1992**, *50*, 629.

20. Gitler, M. S.; de la Cruz, R.; Zeeberg, B. R.; Reba, R. C. *Life Sci.* **1994**, *55*, 1493.

21. McRee, R. C.; Boulay, S. F.; Sood, V. K.; Cohen, E. I.; Cohen, V. I.; Gitler, M. S.; Zeeberg, B. R.; Gibson, R. E.; Reba, R. C. *Neuroimage* **1995**, *2*, 55.

22. Gitler, M. S.; Reba, R. C.; Cohen, V. I.; Rzeszotarski, W. J.; Baumgold, J. *Brain Research* **1992**, *582*, 253.

23. Kiesewetter, D. O.; Silverton, J. V.; Eckelman, W. C. *J. Med. Chem.* **1995**, *38*, 1711.

24. Kaiser, C.; Audia, V. H.; Carter, J. P.; McPherson, D. W.; Waid, P. P.; Lowe, V. C.; Noronha-Blob, L. *J. Med. Chem.* **1993**, *36*, 610.

25. Kiesewetter, D. O.; Flippen-Anderson, J. L.; Eckelman, W. C. *J. Labelled Compd. Radiopharm.* **1995**, *37*, 686.

26. Lee, J. T.; Paik, C. H.; Kiesewetter, D. O.; Park, S. G.; Eckelman, W. C. *Nucl. Med. Biol.* **1995**, *22*, 773.

27. Boulay, S. F.; Sood, V. K.; Rayeq, M. R.; Zeeberg, B. R.; Eckelman, W. C. *Nucl. Med. Biol.* **1996**, *23*, 889.

28. Greene, T. W.; Wuts, P. G. M. *Protecting Groups in Organic Synthesis*; Wiley-Interscience: New York, 1991; p 260.

29. Prenant, C.; Barre, L.; Crouzel, C. *J. Labelled Compd. Radiopharm.* **1989**, *27*, 1257.

30. Berridge, M. S.; Sayre, L. M.; Arora, P. K.; Terris, A. H.; Riachi, N. J.; Harik, S. I. *J. Med. Chem.* **1993**, *36*, 1284.

31. Van Dort, M. E.; Jung, Y.-W.; Sherman, P. S.; Kilbourn, M. R.; Wieland, D. M. *J. Med. Chem* **1995**, *38*, 810.

32. Kiesewetter, D. O.; Lee, J.; Lang, L.; Park, S. G.; Paik, C. H.; Eckelman, W. C. *J. Med. Chem.* **1995**, *38*, 5.

33. Li, M.; Yasuda, R. P.; Wall, S. J.; Wellstein, A.; Wolfe, B. B. *Mol. Pharmacol.* **1991**, *40*, 28.

34. DeGrado, T. R.; Turkington, T.; Williams, J. J.; Hoffman, J. M.; Coleman, R. E. *J. Nucl. Med.* **1994**, *35*, 1398.

(*Received in U.S.A.* 5 *February* 1997; *accepted* 31 *March* 1997)